

J. Hydrol. Hydromech., 67, 2019, 2, 191–200  
DOI: 10.2478/johh-2018-0023

## Using Beerkan experiments to estimate hydraulic conductivity of a crusted loamy soil in a Mediterranean vineyard

Vincenzo Alagna<sup>1</sup>, Vincenzo Bagarello<sup>1</sup>, Simone Di Prima<sup>2\*</sup>, Fabio Guaitoli<sup>3</sup>, Massimo Iovino<sup>1</sup>, Saskia Keesstra<sup>4,5</sup>, Artemi Cerdà<sup>4,6</sup>

<sup>1</sup> Department of Agricultural, Food and Forest Sciences, University of Palermo, Viale delle Scienze, 90128 Palermo, Italy.

<sup>2</sup> Agricultural Department, University of Sassari, Viale Italia, 39, 07100 Sassari, Italy.

<sup>3</sup> Assessorato regionale dell'Agricoltura, dello Sviluppo Rurale e della Pesca Mediterranea, UO S5.05, Viale Regione Siciliana 2771, 90145 Palermo Italy.

<sup>4</sup> Team Soil Water and Land Use, Wageningen Environmental Research, Wageningen UR, Droevendaalsesteeg 3, 6700 AA Wageningen, The Netherlands.

<sup>5</sup> Civil, Surveying and Environmental Engineering, The University of Newcastle, Callaghan 2308, Australia.

<sup>6</sup> Department of Geography, University of Valencia, Blasco Ibáñez, 28, 46010 València, Spain.

\* Corresponding author. E-mail: [sdiprima@uniss.it](mailto:sdiprima@uniss.it)

**Abstract:** In bare soils of semi-arid areas, surface crusting is a rather common phenomenon due to the impact of raindrops. Water infiltration measurements under ponding conditions are becoming largely applied techniques for an approximate characterization of crusted soils. In this study, the impact of crusting on soil hydraulic conductivity was assessed in a Mediterranean vineyard (western Sicily, Italy) under conventional tillage. The BEST (Beerkan Estimation of Soil Transfer parameters) algorithm was applied to the infiltration data to obtain the hydraulic conductivity of crusted and uncrusted soils. Soil hydraulic conductivity was found to vary during the year and also spatially (i.e., rows vs. inter-rows) due to crusting, tillage and vegetation cover. A 55 mm rainfall event resulted in a decrease of the saturated soil hydraulic conductivity,  $K_s$ , by a factor of 1.6 in the inter-row areas, due to the formation of a crusted layer at the surface. The same rainfall event did not determine a  $K_s$  reduction in the row areas (i.e.,  $K_s$  decreased by a non-significant factor of 1.05) because the vegetation cover intercepted the raindrops and therefore prevented alteration of the soil surface. The developed ring insertion methodology on crusted soil, implying pre-moistening through the periphery of the sampled surface, together with the very small insertion depth of the ring (0.01 m), prevented visible fractures. Consequently, Beerkan tests carried out along and between the vine-rows and data analysis by the BEST algorithm allowed to assess crusting-dependent reductions in hydraulic conductivity with extemporaneous measurements alone. The reliability of the tested technique was also confirmed by the results of the numerical simulation of the infiltration process in a crusted soil. Testing the Beerkan infiltration run in other crusted soils and establishing comparisons with other experimental methodologies appear advisable to increase confidence on the reliability of the method that seems suitable for simple characterization of crusted soils.

**Keywords:** Hydraulic conductivity; Water infiltration measurements; Soil surface crust; Vineyard; BEST procedure.

### INTRODUCTION

The impact of raindrops on a bare soil surface can result in physical and chemical changes of the exposed soils. The mechanical alteration of the upper soil aggregates can determine development of a surface crust (Assouline, 2004). This type of crust, named structural crust, differs from a depositional crust (West et al., 1992), which is formed by deposition of detached, fine particles transported in suspension by runoff (Fox et al., 1998). The hydraulic properties of crusts vary significantly as compared with the non-altered soil (Fox et al., 1998). Different physical rainfall properties may be related with structural crust development, such as intensity (Freebairn et al., 1991), kinetic energy (Eigel and Moore, 1983) and momentum (Brodie and Rosewell, 2007; Rose, 1960). The initial or wetting phase in crust formation is defined as surface sealing (Römken, 1979). During the drying cycle, this layer consolidates and may differ from the wetting phase in its mechanical and hydraulic properties (Mualem et al., 1990). This drying phase is known as crusting (Römken, 1979).

The hydrodynamic properties of such a layered system (crust layer, underlying soil) may severely affect the partition between infiltration and runoff at the soil surface, especially in arid

and semi-arid areas where crusting is a common phenomenon (Angulo-Jaramillo et al., 2016; Assouline, 2004). Water infiltration measurements are becoming common for an indirect characterization of sealed/crusted soils (Bedaiwy, 2008). For instance, Vandervaere et al. (1997) developed a field method using a tension infiltrometer and a minitensiometer inserted laterally at the crust-underlying soil interface. The minitensiometer is used to detect the arrival of the wetting front and thus to separate the water infiltration in the crust solely from that in the entire crust-soil medium. However, minitensiometer installation may be problematic, especially for crust layer thinner than 1 cm. Moreover, in crusts with high surface roughness, some issue may be encountered to ensure the hydraulic contact between the disk and the surface crust.

The Beerkan Estimation of Soil Transfer (BEST) parameters procedure developed by Lassabatere et al. (2006) is a very attractive method for practical use since it allows an estimation of both the soil water retention and hydraulic conductivity functions. The BEST method focuses specifically on the van Genuchten (1980) relationship for the water retention curve with the Burdine (1953) condition and the Brooks and Corey (1964) relationship for hydraulic conductivity. BEST estimates shape parameters of the assumed relationships, which are tex-

ture dependent, from particle-size analysis by physical-empirical pedotransfer functions, and scale parameters from Beerkan experiments (Haverkamp et al., 1996), i.e. three-dimensional (3D) field infiltration experiments at ideally zero pressure head. Following Reynolds and Elrick (2005), ring infiltration data are essentially representative of vertical soil water transmission parameters since rings establish downward flow. BEST substantially facilitates the hydraulic characterization of unsaturated soils, and it is gaining popularity in soil science (e.g., Di Prima et al., 2018b; Gonzalez-Sosa et al., 2010). Alternative algorithms, i.e., BEST-slope (Lassabatere et al., 2006), BEST-intercept (Yilmaz et al., 2010) and BEST-steady (Bagarello et al., 2014b), and field procedures based on BEST method were developed (Alagna et al., 2016). The ability of the BEST method to assess the effect of surface crust on the soil hydraulic properties was demonstrated by Souza et al. (2014) in a cropped soil located in the north-eastern region of Brazil. Moreover, Di Prima et al. (2017, 2018a) successfully applied a Beerkan experiment involving different heights of water pouring on the infiltration surface to explain surface runoff and sealing generation phenomena occurring during intense rainfall events. These authors concluded that if any seal forms at the surface, the Beerkan infiltration test should detect its impact on flow and BEST estimates should essentially indicate the hydraulic properties of the surface layer. In fact, the BEST method was developed for non-layered soils that are assumed to be uniform and have a uniform soil water content at the beginning of the infiltration run (Lassabatere et al., 2006, 2009) and should not contain a macropore network (Lassabatere et al., 2014). However, completely homogeneous soils are very rare in natural environments (Reynolds and Elrick, 2002). Therefore, the hydraulic conductivity obtained by an infiltrometer method, such as BEST, should probably be considered as an equivalent conductivity, i.e. the conductivity of a rigid, homogeneous and isotropic porous medium characterized by infiltration rates that are the same as those actually measured on the real soil (Bagarello et al., 2010). For the case of stratified media, the layer with the lowest hydraulic conductivity generally controls the flow and, consequently, cumulative infiltration at the surface (Alagna et al., 2013). Therefore, water infiltration data can be regarded as representative of the hydraulic behavior of the least permeable layer, and therefore the derived BEST parameters can be assigned to this layer. This approach was proposed by Lassabatere et al. (2010) for a stratified medium with a low permeability sedimentary layer at the surface, Yilmaz et al. (2013, 2010) for the characterization of crusted reactive materials and, recently, Coutinho et al. (2016) for a permeable pavement for stormwater management in an urban area. Although Souza et al. (2014) firstly demonstrated the ability of BEST to properly characterize a crusted soil, testing this assumption is necessary to assess the real potential of BEST for the case of a soil with a fine layering organization. In other words, while discrepancies between crusted and no-crusted soils are expected to be detected by the BEST procedure, in the scientific literature there is no exhaustive testing of the BEST capacity to yield reliable hydraulic properties of the crust layer solely.

In this paper we tested the BEST method in an agricultural setting with the general objective to carry out a hydraulic characterization of a loamy soil in a vineyard under conventional tillage located at Marsala (western Sicily, Italy). In particular, both row and inter-row areas were sampled since a crust layer only developed in the latter area. Therefore, the specific objective was to check the ability of the BEST method to yield plausible estimates of saturated hydraulic conductivity of crusted

and non-crusted soils. The ability of the proposed technique to give a hydraulic characterization of the surface crust was then assessed by numerical simulation of the infiltration process in the two-layer system formed by the crust and the underlying soil.

## MATERIAL AND METHODS

### Study site

The experimental site is located close to Marsala (western Sicily, Italy), in the homeland of Sicilian viticulture (37°48'5.10" N and 12°30'44.79" E). Elevation is 111 m a.s.l. and soil surface is flat. The soil is a typical Rhodoxeralf with a depth of 1 m and a small amount of gravel. According to USDA classification, the soil texture, determined on two replicated soil samples, is loam (Table 1). A weather station is located 5 km away from the sampling site (37°79'35.64"N and 12°56'81.59"E). It is positioned at the same elevation as the sampling site and it is part of a network of stations managed by Servizio Informativo Agrometeorologico Siciliano – SIAS.

**Table 1.** Clay (%), silt (%) and sand (%) content (Soil Survey Staff, 2014), soil textural classification, hydraulic shape parameters  $m$ ,  $n$  and  $\eta$  (–), dry soil bulk density,  $\rho_b$  ( $\text{g cm}^{-3}$ ), and saturated soil water content,  $\theta_s$  ( $\text{cm}^3\text{cm}^{-3}$ ), of the sampled vineyard soil. Coefficient of variation (%) in brackets.

Variable	Site characteristic
clay	19.7
silt	49.6
sand	30.7
textural classification	loam
$m$	0.079
$n$	2.172
$\eta$	14.6
$\rho_b$	1.128 (5.1)
$\theta_s$	0.575 (3.8)

At the experimental site, the common soil management for the vineyards of Marsala was applied during the two years of sampling (2015 and 2016) (Figure 1). The soil is tilled to a depth of 0.10–0.15 m in October, after the first autumn rainfalls. Faba bean (*Vicia faba* L. var. *minor*) is sown in November between the rows. In March, the legume biomass is cut and immediately incorporated into the soil with a rotary tiller to a depth of 0.20 m. Finally, a new rotary tillage is performed in May and, only for the second year, this was also done in June. This soil management practice is applied between the rows. Along the rows, a mechanical topper is used at each soil tillage date to a depth of 0.10 m.

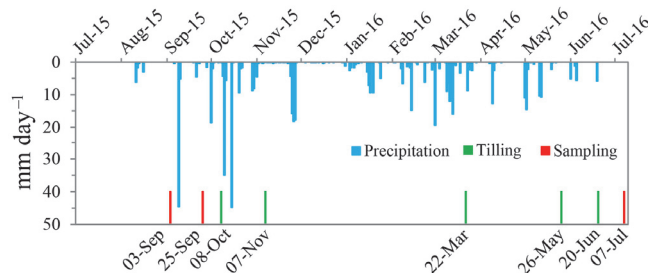


**Fig. 1.** Precipitation and soil management program during the study period. The sampling dates are reported.

## Soil sampling

An area of approximately 100 m<sup>2</sup> was sampled on three different sampling campaigns covering two growing seasons. The first two campaigns were carried out at the beginning and the end of September 2015, respectively, and the third campaign was performed at the beginning of July 2016. Between the first two sampling campaigns, the soil was left bare and not tilled, and a total rainfall of 55 mm fell (Figure 1), which is approximately 10% of the average annual precipitation for the area. In particular, a 29-mm event occurred during the morning of 9 September, with a maximum recorded intensity of 25 mm h<sup>-1</sup>. During the same day, a total of 44.6 mm of precipitation was recorded. This rainfall led to the development of a weak but clearly detectable surface crust (thickness of ~4 mm) (Figure 2). This phenomenon was only observed between the rows and not along the rows. The second sampling was done one week after the last rainfall event. Finally, a third sampling campaign was carried out during the following dry season in order to sample the soil after the ordinary tillage practices and with moisture conditions comparable to the first sampling date.

On each sampling date, a total of 10 undisturbed soil cores (5 cm in height by 5 cm in diameter) were collected at the soil surface close to the points where the infiltration tests were performed, 5 along the rows and 5 between the rows. These cores were used to determine the dry soil bulk density,  $\rho_b$  (g cm<sup>-3</sup>), and the soil water content at the time of the experiment,  $\theta_i$  (cm<sup>3</sup> cm<sup>-3</sup>). The soil porosity was calculated from the  $\rho_b$  data, assuming a soil particle density of 2.65 g cm<sup>-3</sup>. A disturbed soil sample (0–10 cm depth), collected both along and between the rows, was used to determine the particle size distribution (PSD), using conventional methods (Gee and Bauder, 1986). Fine size fractions were determined by the hydrometer method, whereas the coarse fractions were obtained by mechanical dry sieving. The clay, silt and sand percentages were determined from the measured PSD according to USDA standards.

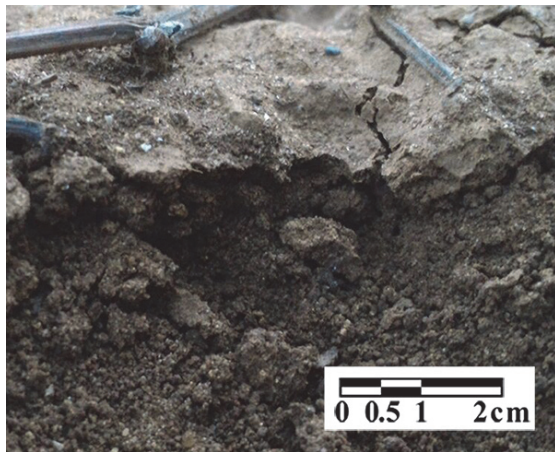


**Fig. 2.** Surface crust layer developed after the intense storms fallen the 9<sup>th</sup> of September 2015, and encountered on the soil surface between the vineyard rows during the second field campaign (see Figure 1). Photo by V. Alagna.

## Beerkan experiments

For each sampling date, an area of approximately 100 m<sup>2</sup> was chosen and 14 Beerkan infiltration runs (Lassabatere et al., 2006) were carried out using a 15 cm inner-diameter ring. Seven runs were carried out along the rows and seven on the bare inter-rows area. The steel ring was positioned between two vine

stocks along the row and in the same orthogonal direction between the rows. The ring was inserted to a depth of about 0.01 m into the soil surface to avoid lateral loss of the ponded water. On crusted soil, to prevent fracture of the upper layer during ring insertion, the soil outside the hedge of the ring was moistened with 5 cm<sup>3</sup> of water by means of a syringe before insertion. Due to the very limited thickness of the crust, insertion of the minitensiometer requested by the Vandervaere et al. (1997) method would have been problematic resulting in disruption of the crust. After ten minutes, the ring was carefully inserted to the pre-established short depth applying a slight pressure and a gentle rotation. This site preparation was essential to prevent visible crust surface perturbation.

According to the guidelines by Lassabatere et al. (2006), for each run a known volume of water (150 mL) was poured in the cylinder at the start of the experiment and the elapsed time during its infiltration was measured. When the amount of water had completely infiltrated, another identical volume of water was poured on the confined infiltration surface and the time needed for the complete infiltration was logged. The procedure was repeated 15 times for each run by applying water at a small distance (3 cm of height) from the infiltration surface. As is commonly suggested in practical application of a ponding infiltration method, the energy of the water due to the application was dissipated on the fingers of a hand in order to minimize soil disturbance (Reynolds, 2008).

As mentioned before, BEST focuses specifically on the following relationships to describe the water retention curve (Burdine, 1953; van Genuchten, 1980) and the hydraulic conductivity function (Brooks and Corey, 1964):

$$\frac{\theta - \theta_r}{\theta_s - \theta_r} = \left[ 1 + \left( \frac{h}{h_g} \right)^n \right]^{-m} \quad (1a)$$

$$m = 1 - \frac{2}{n} \quad (1b)$$

$$\frac{K(\theta)}{K_s} = \left( \frac{\theta - \theta_r}{\theta_s - \theta_r} \right)^\eta \quad (2a)$$

$$\eta = \frac{2}{n \times m} + 3 \quad (2b)$$

where  $\theta$  (cm<sup>3</sup> cm<sup>-3</sup>) is the volumetric soil water content,  $\theta_r$  (cm<sup>3</sup> cm<sup>-3</sup>) is the residual volumetric soil water content,  $\theta_s$  (cm<sup>3</sup> cm<sup>-3</sup>) is the saturated volumetric soil water content,  $h_g$  (mm) is the van Genuchten pressure scale parameter,  $K$  (L T<sup>-1</sup>) is the soil hydraulic conductivity, and  $n$ ,  $m$  and  $\eta$  are shape parameters linked to the soil textural properties. In BEST, these last parameters are estimated from the analysis of the PSD with the pedotransfer function included in the procedure. Taking into account that a low spatial and temporal variability is expected for soil texture at the field scale (Warrick, 1998), representative values of the shape parameters for the field site were obtained by averaging the individual determinations (Table 1). BEST considers  $\theta_r$  to be zero, and  $\theta_s$  was assumed to coincide with soil porosity in this investigation, as suggested by many authors (e.g., Castellini et al., 2018; Coutinho et al., 2016; Di Prima, 2015; Mubarak et al., 2010, 2009; Xu et al., 2009; Yilmaz et al., 2010). Moreover, Di Prima et al. (2017) demonstrated that the assumed coincidence between saturated soil water content and porosity affects only marginally  $K_s$  estimation.

BEST-slope estimates sorptivity,  $S$  ( $\text{mm h}^{-0.5}$ ), by fitting the experimental cumulative infiltration data on the explicit transient two-term equation by Haverkamp et al. (1994):

$$I(t) = S\sqrt{t} + \left[ A(1-B)S^2 + Bi_s \right] t \quad (3)$$

where  $I$  (mm) is 3D cumulative infiltration and  $t$  (h) is the time. Then,  $K_s$  ( $\text{mm h}^{-1}$ ) is estimated as a function of  $S$  as follow:

$$K_s = i_s - AS^2 \quad (4)$$

where  $i_s$  ( $\text{mm h}^{-1}$ ) is the experimental steady-state infiltration rate, which is estimated by linear regression analysis of the last data points describing steady-state conditions on the  $I$  vs.  $t$  plot and corresponds to the slope of the regression line. The constants  $A$  ( $\text{mm}^{-1}$ ) and  $B$  can be defined for the specific case of a Brooks and Corey relation (Eq. 2) and taking into account initial soil water content,  $\theta_i$  ( $\text{cm}^3 \text{cm}^{-3}$ ), as (Haverkamp et al., 1994):

$$A = \frac{\gamma}{r(\theta_s - \theta_i)} \quad (5a)$$

$$B = \frac{2-\beta}{3} \left[ 1 - \left( \frac{\theta_i}{\theta_s} \right)^\eta \right] + \left( \frac{\theta_i}{\theta_s} \right)^\eta \quad (5b)$$

where  $\gamma$  (parameter for geometrical correction of the infiltration front shape) and  $\beta$  are coefficients that are commonly set at 0.75 and 0.6, respectively, for  $\theta_i < 0.25 \theta_s$ , and  $r$  (mm) is the radius of the source. Finally,  $h_g$  is estimated by the following relationship (Lassabatere et al., 2006):

$$h_g = - \frac{S^2}{c_p(\theta_s - \theta_i) \left[ 1 - \left( \frac{\theta_i}{\theta_s} \right)^\eta \right] K_s} \quad (6)$$

where:

$$c_p = \Gamma \left( 1 + \frac{1}{n} \right) \left\{ \frac{\Gamma \left( m\eta - \frac{1}{n} \right)}{\Gamma(m\eta)} + \frac{\Gamma \left( m\eta + m - \frac{1}{n} \right)}{\Gamma(m\eta + m)} \right\} \quad (7)$$

in which  $\Gamma$  stands for the Gamma function.

### Numerical simulations

Numerical simulations of the infiltration process were carried out to assess the ability of the Beerkan method to distinguish between crusted and non-crusted soils. In particular, the assumption was tested that the crust layer can be characterized by the parameters derived by BEST. The numerical simulations were carried out using the graphical software package VS2DI (Healy and Ronan, 1996), developed by the U.S. Geological Survey for simulating the movement of water and transport of solute or heat in variably saturated porous media. In particular, the finite-difference method was used to solve the Richards equation for water flow. According to Nasta et al. (2012), a zero pressure head boundary condition was imposed on the soil surface delimited by the ring, while free drainage was set at the

bottom of the modeled domain. The BEST derived parameters were used in VS2DI to obtain the simulated cumulative infiltration curves. In particular, the parameters estimated along the row and on the bare inter-row area during the second field campaign (i.e., after development of a crusted layer in the latter area) were used to define the hydraulic properties of the underlying soil and the crust layer (thickness of 4 mm), respectively. Moreover, with the aim to assess the impact of the hydraulic conductivity of the crust layer on the simulated curves, different  $K_s$  values of the crust layer (from 94 to 166  $\text{mm h}^{-1}$ ) were considered. This range was established by considering the experimental  $K_s$  value for the crust layer plus or minus approximately 30% of this value. Then, the simulated cumulative infiltration curves ( $I_{SIMULATION}$ ) were compared with the mean experimental infiltration curve obtained on the crusted soil during the second field campaign ( $I_{BEST}$ ) using the root mean square error (RMSE):

$$RMSE = \sqrt{\frac{\sum_{i=1}^N [I_{SIMULATION}(t_i) - I_{BEST}(t_i)]^2}{N}} \quad (8)$$

where  $N$  is the total number of data pairs (15 in this investigation), and  $t_i$  is the time required for the infiltration of a given water depth.

### Data analysis

Data sets were summarized by calculating the mean,  $M$ , and the associated coefficient of variation,  $CV$ . In particular, the  $cl$ ,  $si$ ,  $sa$ ,  $\rho_b$ , and  $\theta_s$  values were assumed to be site specific and therefore they were determined only in duplicate ( $cl$ ,  $si$ ,  $sa$ ,  $N=2$ ) or, considering their low variability ( $\rho_b$ ,  $\theta_s$ ), the arithmetic mean and the associated  $CV$  were calculated (Table 1). Temporal variability of  $\theta_i$  was determined on the basis of ten replicate samples on each sampling date (Table 2).

**Table 2.** Minimum (Min), maximum (Max), mean, and coefficient of variation (CV, in %) of the soil water content at the time of sampling,  $\theta_i$  ( $\text{cm}^3 \text{cm}^{-3}$ ), values for different sampling dates (sample size  $N=10$  for each sampling date).

Statistic	Sept 3, 2015	Sept 25, 2015	Jul 7, 2016
Min	0.051	0.093	0.047
Max	0.073	0.133	0.087
Mean	0.064 A	0.114 B	0.067 A
CV	12.0	10.9	18.1

The values in a row followed by the same upper case letter were not significantly different according to the Tukey Honestly Significant Difference test ( $P < 0.05$ ). The values followed by a different upper case letter were significantly different.

Sorptivity values were assumed normally distributed. The  $K_s$  and  $h_g$  data were assumed to be log-normally distributed since the statistical distribution of these data is generally log-normal (Lee et al., 1985; Warrick, 1998). The geometric mean and the associated  $CV$  were therefore calculated to summarize  $K_s$  and  $h_g$  values using the appropriate “log-normal equations” (Lee et al., 1985). Statistical comparison between two sets of data was conducted using two-tailed t-tests, whereas the Tukey Honestly Significant Difference test was applied to compare three sets of data. The ln-transformed  $K_s$  and  $h_g$  data were used in the statistical comparison. A probability level,  $P < 0.05$ , was used for all statistical analyses. Since a fitting of the infiltration model to the transient data is required with BEST, the quality of the fit was evaluated by controlling both the general shape and the

relative error defined as (Lassabatere et al., 2006):

$$Er = \sqrt{\frac{\sum_{i=1}^k [I^{\text{exp}}(t_i) - I_{\text{est}}(t_i)]^2}{\sum_{i=1}^k I^{\text{exp}}(t_i)^2}} \quad (9)$$

where  $k$  is the number of data points considered for the transient state,  $I^{\text{exp}}$  is the experimental cumulative infiltration and  $I_{\text{est}}$  is the estimated cumulative infiltration using Eq. (3).

## RESULTS AND DISCUSSION

### Impact of surface crusting on soil hydraulic properties

The 42 infiltrations runs analyzed with the BEST-slope algorithm yielded plausible, i.e. positive,  $K_s$  values in all cases. In addition, the fitting of the infiltration model to the transient phase of the infiltration run always yielded low relative errors, denoting an acceptable approximation for transient cumulative infiltration according to the criterion proposed by Lassabatere et al. (2006) (Figure 3).

During the second field campaign, crusting phenomena, affecting water infiltration, were only detected between the rows. The protective role of vegetation along the rows was therefore effective, intercepting raindrops and preventing surface sealing (Dunne et al., 1991). The protective role along the vine-rows is well known, while in vine inter-rows the mulching practice is commonly applied to protect soil from raindrop impact (Celette et al., 2008). For the second campaign, the mean  $K_s$  value obtained between the rows was 1.64 times lower than the one obtained along the rows (Table 3). This latter value, equal to

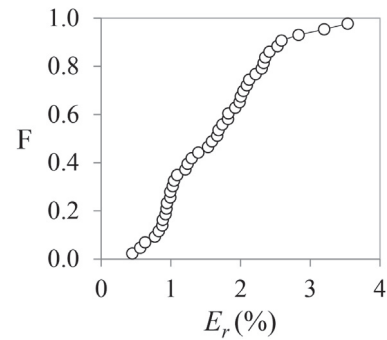


**Fig. 3.** Cumulative frequency distribution of the relative errors,  $E_r$  (%), of the fitting of the infiltration model to the transient phase of the infiltration runs.

212.4 mm h<sup>-1</sup>, did not significantly differ from those of the first and third sampling dates. In addition, during the first and third campaigns, Beerkan runs carried out along and between the rows yielded similar  $K_s$  values, due to the absence of a crust between the rows. This experimental information suggested that cover influenced crusting development and consequently both the temporal and the spatial variation of the soil hydrological characteristics at the field site.

Bradford et al. (1987) reported for 20 soils varying in texture from sand to clay a reduction in infiltration rate after 60 min of simulated rainfall (intensity of 63 mm h<sup>-1</sup>), due to the effect of surface sealing on infiltration. Bagarello et al. (2014a), Alagna et al. (2016) and Di Prima et al. (2017) applied on five soils having different texture a BEST derived procedure to explain surface runoff and disturbance phenomena at the soil surface

**Table 3.** Minimum (Min), maximum (Max), mean, and coefficient of variation (CV, in %) of the saturated soil hydraulic conductivity,  $K_s$  (mm h<sup>-1</sup>), soil sorptivity,  $S$  (mm h<sup>-0.5</sup>), and the water pressure scale parameter,  $h_g$  (mm), values obtained from BEST experiments carried out along and within the rows on different sampling dates (sample size  $N = 7$  for each variable and each date).

Variable	Rows/Inter-rows	Statistic	Sept 3, 2015	Sept 25, 2015	Jul 7, 2016
$K_s$	Rows	Min	188.1	159.1	158.4
		Max	289.1	369.1	234.2
		Mean	223.6 a A	212.4 a A	199.2 a A
		CV	15.4	27.6	14.1
	Inter-rows	Min	193.0	97.0	160.6
		Max	261.8	251.3	272.3
		Mean	229.5 a A	129.3 b B	192.5 a A
		CV	10.3	31.7	20.2
$S$	Rows	Min	105.5	84.0	87.7
		Max	130.6	99.8	112.9
		Mean	114.3 a A	94.4 a B	99.3 a B
		CV	6.8	5.6	9.1
	Inter-rows	Min	107.2	74.3	86.7
		Max	120.8	97.8	96.8
		Mean	113.5 a A	84.3 b B	91.2 b B
		CV	3.5	8.6	4.4
$h_g$	Rows	Min	-56.4	-50.3	-53.9
		Max	-40.1	-24.0	-32.3
		Mean	-47.7 a A	-37.9 a A	-40.7 a A
		CV	11.2	27.8	20.1
	Inter-rows	Min	-51.4	-66.8	-43.6
		Max	-40.8	-27.7	-23.7
		Mean	-45.8 a AB	-49.6 a A	-35.5 a B
		CV	9.3	31.5	19.7

For a given variable, the values in the column followed by a different lower case letter were significantly different according to a two tailed t test ( $P < 0.05$ ). The values in a row followed by a different upper case letter were significantly different according to the Tukey Honestly Significant Difference test ( $P < 0.05$ ).

occurring during intense rainfall events. These authors reported  $K_s$  values of the disturbed soil from nine to 33 times lower than the undisturbed soils. In particular, Di Prima et al. (2017) applied this methodology in a vineyard with a sandy-loam texture. These authors compared this simple methodology with rainfall simulation experiments establishing a physical link between the two methodologies through the kinetic energy of the rainfall and the gravitational potential energy of the water used for the Beerkan runs. They also indirectly demonstrated the occurrence of a certain degree of compaction and mechanical breakdown using a mini disk infiltrometer (Decagon, 2014). With this device, they reported a reduction of the unsaturated hydraulic conductivity by 2.3 times due to the seal formation. In another investigation carried out in Brazil with the BEST procedure, non-crustured soils were three times more conductive than the crustured soil (Souza et al., 2014).

Although this investigation was essentially focused on soil hydraulic conductivity, an analysis of the  $S$  and  $h_g$  parameters was carried out since they also depend on the measured infiltration curve. The means of soil sorptivity varied from 84.3 to 114.3 mm h<sup>-0.5</sup> (difference by a factor of 1.36) and the associated  $CV$ s ranged from 3.5% to 9.1% (Table 3). In all cases (sampling dates, position), relative variability was smaller for  $S$  than for  $K_s$ . This result was considered physically plausible. In fact,  $S$  is more expressive of the capillary forces exerted by the soil matrix, which are known not to vary much in space. Therefore, the estimates of  $S$  appeared plausible on the basis of the physical meaning of this variable (Alagna et al., 2016). Slightly but significantly lower  $S$  values were obtained during the last two sampling dates. During the first field campaign similar  $S$  values were obtained at the two positions, whereas during the second field campaign the effect of the crust layer on  $S$  was statistically significant although not very noticeable because the mean of  $S$  obtained between the rows was only 1.12 times lower than that obtained along the rows. Therefore, the crust layer determined a reduced ability of the porous medium to adsorb water due to capillarity (Alagna et al., 2016). This last effect was not persistent since the differences between the row and the inter-row area were smaller on the third sampling date. However, the sign of a decrease with time of the differences between means of  $S$  was weak since the factor of difference decreased only from 1.12 to 1.09.

The means of the pressure scale parameter varied from -49.6 to -35.5 mm (difference by a factor of 1.4) and the associated  $CV$ s ranged from 9.3% to 31.5% (Table 3). The  $h_g$  parameter is expected to be smaller (more negative) for a crust than for the underlying soil due to compaction and dispersion of fine material from aggregates (Smith, 1990). However, in this investigation the presence of a crust did not clearly affect the  $h_g$  parameter. As a matter of fact, a smaller  $h_g$  value in the inter-row area than the row area was only detected on the second sampling date, i.e. when a crust layer developed in the former zone. However, the  $h_g$  differences were not statistically significant.

### Seasonal dynamics in hydraulic conductivity

For the first and the third campaign, the Beerkan runs carried out between the rows (inter-row areas) yielded comparable and statistically similar  $K_s$  values (Table 3). In both cases, the average  $K_s$  values were approximately 20 times higher than the expected saturated conductivity on the basis of the soil textural characteristics alone (e.g.,  $K_s = 10.4$  mm h<sup>-1</sup> for a loam soil according to Carsel and Parrish, 1988). This circumstance suggested that soil macroporosity generated by soil tillage in the ploughed horizon likely influenced measurement of  $K_s$

(Alagna et al., 2016; Di Prima et al., 2017; Josa et al., 2010). In these conditions, the soil structure is expected to be particularly fragile, especially with reference to macroporosity, and hence unstable (Jarvis et al., 2008), which implies that clogging of the largest pores at the soil surface, as a consequence of the aggregates breakdown occurring during a rainstorm, can easily mitigate tillage effects on soil hydraulic properties (Ciollaro and Lamaddalena, 1998).

As discussed in the former section, the presence of the crust layer during the second field campaign clearly affected water infiltration between the rows. In particular, the presence of this layer implied that  $K_s$  was 1.5–1.8 times lower than that measured in the absence of the crusted layer. Crusting at the soil surface determined an increased hydraulic resistance to water penetration into soil (Alagna et al., 2013) since differences between the  $K_s$  datasets (second against both first and third sampling campaigns) were statistically significant. Crusting also resulted in a decrease of the lowest measurable  $K_s$  values, while the highest values remained unchanged (Table 3).

The tillage practices carried out in the spring 2016 removed any existing soil crust and thereby increased soil infiltration properties (Chahinian et al., 2006), suggesting a cycling occurrence of crusting phenomena within the year.

Many studies in the literature have reported similar dynamics, even in vineyards. In fact, infiltration experiments constitute an indirect measurement closely associated with sealing or crusting (Römken et al., 1990), and the saturated hydraulic conductivity may vary considerably during the year if these phenomena occur. In particular, rainfall and wetting–drying cycles favor soil reconsolidation and soil-surface sealing or crusting, whereas tillage removes existing layering (Pare et al., 2011). For instance, Biddoccu et al. (2017) studied temporal variability of soil hydraulic properties in a vineyard on a silt loam soil. These authors reported hydraulic conductivity values measured during the summer four times lower than those measured during the wet season, due to the presence of a structural crust resulting from rainfall events following a long time after the last spring tillage.

### Numerical validation

Figure 4 summarizes the numerical validation exercise that was carried out in this investigation. The smallest  $RMSE$  value was obtained for a crust layer having  $K_s = 133.2$  mm h<sup>-1</sup>. This value differed by a negligible factor of 1.03 from the in situ  $K_s$  value obtained on the layered system (crust layer, underlying soil; Table 3). Figure 4 also shows the comparison between the experimental cumulative infiltration curve and those simulated by assuming a non-layered system, i.e. all crust or all non-altered soil. The vertical homogeneity hypothesis yielded 3.6 to 6.3 times higher  $RMSE$  values as compared with the more realistic soil layering hypothesis. Both simulations (Figures 4b and 4c) supported the hypothesis that the experimental  $K_s$  value of 129 mm h<sup>-1</sup> was representative of the hydraulic behavior of the least permeable layer (i.e., the crust layer). Therefore, the derived BEST parameters could properly be assigned to this layer, which controlled the flow and consequently cumulative infiltration of the stratified medium.

The results reported in this investigation were in agreement with those by Souza et al. (2014) and their suggestion that the Beerkan-based methodology should be usable to distinguish between crusted and non-crustured soils. Indeed, the hydrodynamic properties of both the crust and the underlying soil play a key role during a rainstorm, affecting the partition between infiltration and runoff (Assouline and Mualem, 2006, 2002).

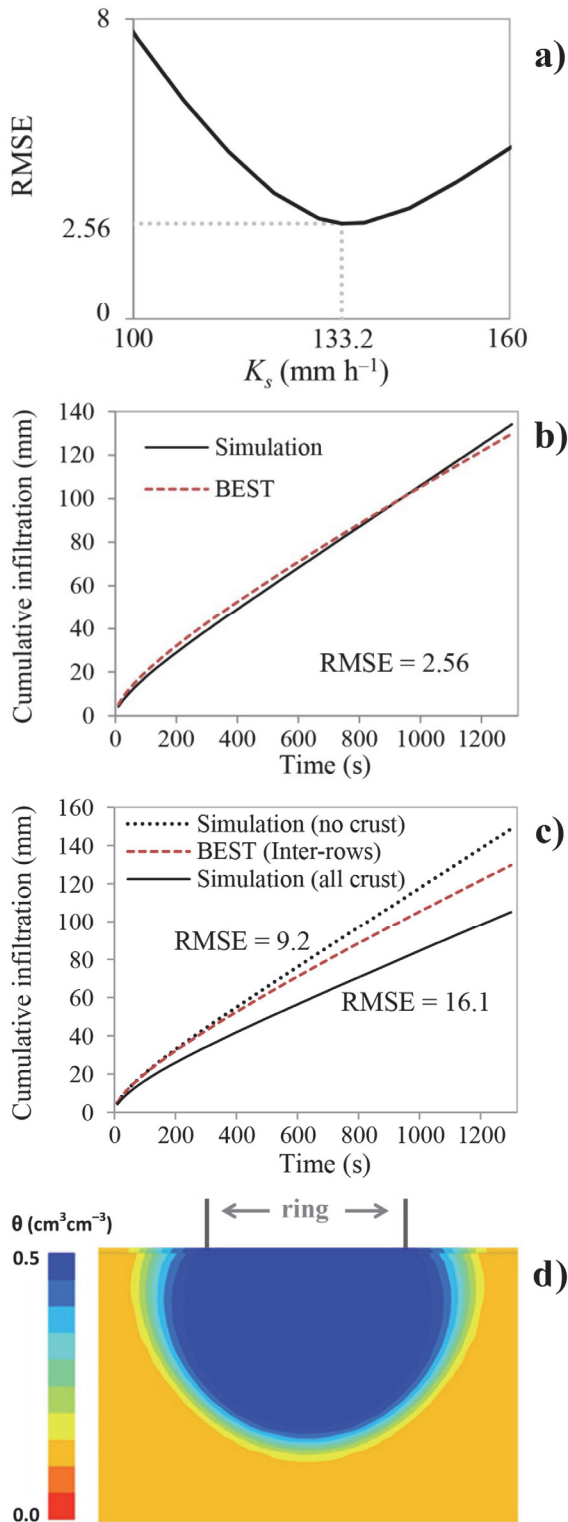


**Fig. 4.** (a) Root mean square error (RMSE) between the simulated and the experimental BEST curves vs. saturated soil hydraulic conductivity,  $K_s$ , values of the surface crust. (b) Infiltration curve simulated with a  $K_s$  value of the surface crust equal to 133.2  $\text{mm h}^{-1}$  (line) compared with the measured curve on the second field campaign in the inter-row area (dashed line). (c) Infiltration curves simulated considering a vertically homogeneous soil profile (dotted and solid lines) compared with the measured curve on the second field campaign in the inter-row area (dashed line). (d) Soil water content profile simulated with  $K_s = 133.2$   $\text{mm h}^{-1}$  at the soil surface.

However, transient methods, as the Beerkan one, appears appropriate to characterize crusted soils, since the properties of the surface layer play a major role at early stages of the infiltration process (Vandervaere et al., 1997). Recently, Di Prima et al. (2016) showed that BEST-slope is less sensitive to the attainment of steady-state and allows to obtain accurate estimates of saturated soil hydraulic conductivity with less water and hence shorter experimental times than the other two BEST algorithms. For these reasons, BEST-slope appears more suitable, among the alternative algorithms, to characterize a crust layer.

#### Hydraulic conductivity functions

Two different approaches were applied in this investigation to check the ability of the BEST procedure to yield a different information between crusted and non-crusted soil. The first approach considered temporal changes of  $K_s$  values obtained between the rows before and after the intense storms fallen in September 2015 that led to the development of a weak but clearly detectable surface crust. As discussed above, with this approach, the third field campaign allowed us to detect the restoring of higher  $K_s$  values because tillage removed the crust. Figure 5a depicts the soil hydraulic conductivity functions obtained from averaged parameters for the different sampling dates at the vine inter-row area. While the curves of the first and the third sampling dates are close to one another, the curve of the second campaign departs from them rather clearly. Indeed, this result could be viewed as a suggestion that this latter curve might represent a crust layer characteristic curve. The second approach, developed with reference to the second sampling date, considered the spatial variation (i.e., rows vs. inter-rows) of conductivity, i.e. taking into account the protective role of the vegetation. A shift between the hydraulic conductivity functions for the row and inter-row areas was also detected, with the soil of the latter area denoting a reduced ability to conduct water for a given soil water content value (Figure 5b). Therefore, both approaches suggested that the BEST procedure was appropriate to show the impact of crusting on soil hydraulic conductivity.

#### Applicability of the Beerkan runs for the assessment of the crusted soil

A perplexity on the possibility to collect reliable data on crusted soils by a ponding infiltration experiment is related to the need to insert the ring into the soil. The doubt is that ring insertion could determine fractures in the crusted layer and these fractures could directly connect the ponded depth of water during the run with the underlying, non-crusted, soil layer (Vandervaere et al., 1997). In other terms, ring insertion could impede, in practice, measurement of fluxes through the crusted layer. In this investigation, fractures were not visually detected at the soil surface, perhaps because the soil was not very dry when the experiment on the crusted layer was performed (Table 2), the ring insertion depth was small (0.01 m), and insertion was carried out a few minutes after moistening the insertion circumference. Other ponding infiltration techniques, such as the single-ring pressure infiltrometer (Reynolds and Elrick, 1990) or, particularly, the simplified falling head technique (Bagarello et al., 2004), presuppose appreciably deeper insertions of the ring and, consequently, more risk to disrupt or alter the fragile crust layer at the soil surface during ring insertion. Therefore, the Beerkan run seems a more appropriate ponding infiltration run to prevent, or minimize, substantial alteration of

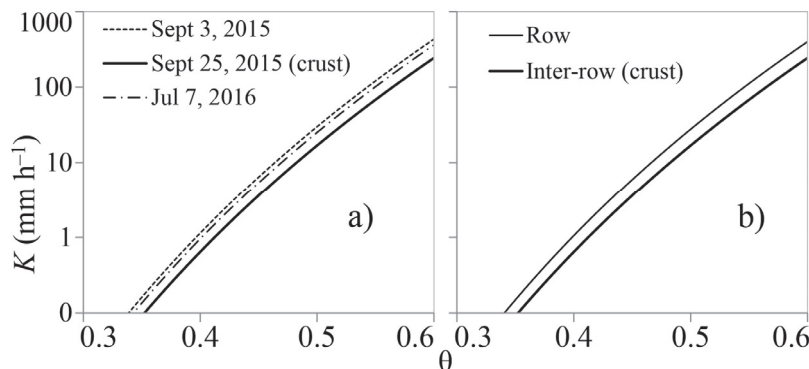


**Fig. 5.** Soil hydraulic conductivity functions obtained from averaged parameters for (a) different sampling dates and (b) along and between the vine-rows.

the surface to be sampled. Obviously, this conclusion needs additional testing but the premises are encouraging, also considering that Beerkan runs were successfully conducted in other crusted soils (Souza et al., 2014). In future application of the method, especially on well-developed crusts, it could be advisable to separately determine the particle size distribution for the crust layer and the subsoil, since alteration of the surface soil layer exposed to rain is known to also induce displacement of fine particles in the vertical direction (Levy et al., 1986).

## CONCLUSIONS

A loam soil was sampled in a Mediterranean vineyard located at Marsala (western Sicily, Italy), with Beerkan infiltration experiments carried out along the rows direction and in the inter-rows during two consecutive growing seasons. Beerkan tests along with BEST-slope algorithm led to plausible estimates of soil hydraulic properties in both crusted and uncrusted conditions, allowing to assess the effect of the cycling occurrence of crusting due to rainfalls and wetting–drying cycles on the vineyard inter-rows.

A sampling strategy implying Beerkan tests carried out along and between the vine-rows was successfully applied. This strategy allowed to assess the reduction in hydraulic conductivity with extemporaneous measurements alone. Its main advantage is that it allows a rapid assessment of crusting severity affecting water infiltration. At the sampled site, the impact of crusting on saturated soil hydraulic conductivity was moderate.

In conclusion, the hypothesis that the Beerkan runs are suitable enough to detect the effect of the crust on flow and BEST estimates appeared reasonable. In the future, the Beerkan-based methodology should be checked in other crusted soils. Comparisons should also be established with other experimental methodologies. The applied methodology in this investigation could be used to explore in the future the functional dynamics of the crust layer under natural rainfall conditions.

*Acknowledgements.* This study was supported by grants from the Research Project CISV (grant n° 2014COMM-0363 CUP 872114000570002). S.D.P. also thanks I.A., E.B. and R.D.O.

## REFERENCES

Alagna, V., Bagarello, V., Di Prima, S., Giordano, G., Iovino, M., 2013. A simple field method to measure the hydrodynamic properties of soil surface crust. *Journal of Agricultural Engineering*, 44, 74–79.

- [https://doi.org/10.4081/jae.2013.\(s1\):e14](https://doi.org/10.4081/jae.2013.(s1):e14)
- Alagna, V., Bagarello, V., Di Prima, S., Giordano, G., Iovino, M., 2016. Testing infiltration run effects on the estimated water transmission properties of a sandy-loam soil. *Geoderma*, 267, 24–33. <https://doi.org/10.1016/j.geoderma.2015.12.029>
- Angulo-Jaramillo, R., Bagarello, V., Iovino, M., Lassabatere, L., 2016. Soils with specific features. In: *Infiltration Measurements for Soil Hydraulic Characterization*. Springer International Publishing, pp. 289–354. [https://doi.org/10.1007/978-3-319-31788-5\\_4](https://doi.org/10.1007/978-3-319-31788-5_4)
- Assouline, S., 2004. Rainfall-induced soil surface sealing. *Vadose Zone Journal*, 3, 570–591.
- Assouline, S., Mualem, Y., 2002. Infiltration during soil sealing: The effect of areal heterogeneity of soil hydraulic properties. *Water Resources Research*, 38, 1286. <https://doi.org/10.1029/2001WR001168>
- Assouline, S., Mualem, Y., 2006. Runoff from heterogeneous small bare catchments during soil surface sealing. *Water Resources Research*, 42, W12405. <https://doi.org/10.1029/2005WR004592>
- Bagarello, V., Iovino, M., Elrick, D., 2004. A Simplified Falling-Head Technique for Rapid Determination of Field-Saturated Hydraulic Conductivity. *Soil Science Society of America Journal*, 68, 66. <https://doi.org/10.2136/sssaj2004.6600>
- Bagarello, V., Stefano, C.D., Ferro, V., Iovino, M., Sgroi, A., 2010. Physical and hydraulic characterization of a clay soil at the plot scale. *Journal of Hydrology*, 387, 54–64. <https://doi.org/10.1016/j.jhydrol.2010.03.029>
- Bagarello, V., Castellini, M., Di Prima, S., Iovino, M., 2014a. Soil hydraulic properties determined by infiltration experiments and different heights of water pouring. *Geoderma*, 213, 492–501. <https://doi.org/10.1016/j.geoderma.2013.08.032>
- Bagarello, V., Di Prima, S., Iovino, M., 2014b. Comparing Alternative Algorithms to Analyze the Beerkan Infiltration Experiment. *Soil Science Society of America Journal*, 78, 724. <https://doi.org/10.2136/sssaj2013.06.0231>
- Bedaiwy, M.N.A., 2008. Mechanical and hydraulic resistance relations in crust-topped soils. *Catena*, 72, 270–281. <https://doi.org/10.1016/j.catena.2007.05.012>
- Biddoccu, M., Ferraris, S., Pitacco, A., Cavallo, E., 2017. Temporal variability of soil management effects on soil hydrological properties, runoff and erosion at the field scale in a hillslope vineyard, North-West Italy. *Soil and Tillage Research*, 165, 46–58. <https://doi.org/10.1016/j.still.2016.07.017>
- Bradford, J.M., Ferris, J.E., Remley, P.A., 1987. Interrill soil erosion processes: I. Effect of surface sealing on infiltration,



- runoff, and soil splash detachment. *Soil Science Society of America Journal*, 51, 1566–1571.
- Brodie, I., Rosewell, C., 2007. Theoretical relationships between rainfall intensity and kinetic energy variants associated with stormwater particle washoff. *Journal of Hydrology*, 340, 40–47. <https://doi.org/10.1016/j.jhydrol.2007.03.019>
- Brooks, R.H., Corey, T., 1964. hydraulic properties of porous media. *Hydrol. Paper 3*. Colorado State University, Fort Collins.
- Burdine, N.T., 1953. Relative permeability calculation from pore size distribution data. *Petr. Trans. Am. Inst. Min. Metall. Eng.* 198, 71–77.
- Carsel, R.F., Parrish, R.S., 1988. Developing joint probability distributions of soil water retention characteristics. *Water Resour. Res.*, 24, 755–769. <https://doi.org/10.1029/WR024i005p00755>.
- Castellini, M., Di Prima, S., Iovino, M., 2018. An assessment of the BEST procedure to estimate the soil water retention curve: A comparison with the evaporation method. *Geoderma*, 320, 82–94. <https://doi.org/10.1016/j.geoderma.2018.01.014>
- Celette, F., Gaudin, R., Gary, C., 2008. Spatial and temporal changes to the water regime of a Mediterranean vineyard due to the adoption of cover cropping. *European Journal of Agronomy*, 29, 153–162. <https://doi.org/10.1016/j.eja.2008.04.007>
- Chahinian, N., Moussa, R., Andrieux, P., Voltz, M., 2006. Accounting for temporal variation in soil hydrological properties when simulating surface runoff on tilled plots. *Journal of Hydrology*, 326, 135–152. <https://doi.org/10.1016/j.jhydrol.2005.10.038>
- Ciollaro, G., Lamaddalena, N., 1998. Effect of tillage on the hydraulic properties of a vertic soil. *Journal of Agricultural Engineering Research*, 71, 147–155. <https://doi.org/10.1006/jaer.1998.0312>
- Coutinho, A.P., Lassabatere, L., Montenegro, S., Antonino, A.C.D., Angulo-Jaramillo, R., Cabral, J.J.S.P., 2016. Hydraulic characterization and hydrological behaviour of a pilot permeable pavement in an urban centre, Brazil. *Hydrol. Process.*, 30, 4242–4254. <https://doi.org/10.1002/hyp.10985>
- Decagon, 2014. *Minidisk Infiltrometer User's Manual*. Decagon Devices, Inc., Pullman, USA, 24 p.
- Di Prima, S., 2015. Automated single ring infiltrometer with a low-cost microcontroller circuit. *Computers and Electronics in Agriculture*, 118, 390–395. <https://doi.org/10.1016/j.compag.2015.09.022>
- Di Prima, S., Lassabatere, L., Bagarello, V., Iovino, M., Angulo-Jaramillo, R., 2016. Testing a new automated single ring infiltrometer for Beerkan infiltration experiments. *Geoderma*, 262, 20–34. <https://doi.org/10.1016/j.geoderma.2015.08.006>
- Di Prima, S., Bagarello, V., Lassabatere, L., Angulo-Jaramillo, R., Bautista, I., Burguet, M., Cerdà, A., Iovino, M., Prosdocimi, M., 2017. Comparing Beerkan infiltration tests with rainfall simulation experiments for hydraulic characterization of a sandy-loam soil. *Hydrological Processes*, 31, 3520–3532. <https://doi.org/10.1002/hyp.11273>
- Di Prima, S., Concialdi, P., Lassabatere, L., Angulo-Jaramillo, R., Pirastru, M., Cerdà, A., Keesstra, S., 2018a. Laboratory testing of Beerkan infiltration experiments for assessing the role of soil sealing on water infiltration. *Catena*, 167, 373–384. <https://doi.org/10.1016/j.catena.2018.05.013>
- Di Prima, S., Rodrigo-Comino, J., Novara, A., Iovino, M., Pirastru, M., Keesstra, S., Cerdà, A., 2018b. Assessing soil physical quality of citrus orchards under tillage, herbicide and organic managements. *Pedosphere*, 28, 3, (in press).
- Dunne, T., Zhang, W., Aubry, B.F., 1991. Effects of rainfall, vegetation, and microtopography on infiltration and runoff. *Water Resour. Res.*, 27, 2271–2285. <https://doi.org/10.1029/91WR01585>
- Eigel, J.D., Moore, I., 1983. Effect of rainfall energy on infiltration into a bare soil. *FAO*.
- Fox, D.M., Le Bissonnais, Y., 1998. Process-based analysis of aggregate stability effects on sealing, infiltration, and interrill erosion. *Soil Science Society of America Journal*, 62, 717–724.
- Fox, D.M., Le Bissonnais, Y., Bruand, A., 1998. The effect of ponding depth on infiltration in a crusted surface depression. *Catena*, 32, 87–100. [https://doi.org/10.1016/S0341-8162\(98\)00042-3](https://doi.org/10.1016/S0341-8162(98)00042-3)
- Freebairn, D.M., Gupta, S.C., Rawls, W.J., 1991. Influence of Aggregate Size and Microrelief on Development of Surface Soil Crusts. *Soil Science Society of America Journal*, 55, 188. <https://doi.org/10.2136/sssaj1991.03615995005500010033x>
- Gee, G.W., Bauder, J.W., 1986. Particle-size analysis. In: Klute, A. (Ed.): *Methods of Soil Analysis, Part 1: Physical and Mineralogical Methods*. SSSA Book Series. Soil Science Society of America, American Society of Agronomy, pp. 383–411.
- Gonzalez-Sosa, E., Braud, I., Dehotin, J., Lassabatère, L., Angulo-Jaramillo, R., Lagouy, M., Branger, F., Jacqueminet, C., Kermadi, S., Michel, K., 2010. Impact of land use on the hydraulic properties of the topsoil in a small French catchment. *Hydrol. Process.*, 24, 2382–2399. <https://doi.org/10.1002/hyp.7640>
- Haverkamp, R., Ross, P.J., Smettem, K.R.J., Parlange, J.Y., 1994. Three-dimensional analysis of infiltration from the disc infiltrometer: 2. Physically based infiltration equation. *Water Resour. Res.*, 30, 2931–2935. <https://doi.org/10.1029/94WR01788>
- Haverkamp, R., Arrúe, J., Vandervaere, J., Braud, I., Boulet, G., Laurent, J., Taha, A., Ross, P., Angulo-Jaramillo, R., 1996. Hydrological and thermal behaviour of the vadose zone in the area of Barrax and Tomelloso (Spain): Experimental study, analysis and modeling. *Project UE n. EV5C-CT 92*, 00-90.
- Healy, R.W., Ronan, A.D., 1996. Documentation of computer program VS2Dh for simulation of energy transport in variably saturated porous media; modification of the US Geological Survey's computer program VS2DT (USGS Numbered Series No. 96-4230), *Water-Resources Investigations Report*. U.S. Geological Survey: Branch of Information Services [distributor].
- Jarvis, N., Etana, A., Stagnitti, F., 2008. Water repellency, near-saturated infiltration and preferential solute transport in a macroporous clay soil. *Geoderma*, 143, 223–230. <https://doi.org/10.1016/j.geoderma.2007.11.015>
- Josa, R., Ginovart, M., Solé, A., others, 2010. Effects of two tillage techniques on soil macroporosity in sub-humid environment. *Int. Agrophys.*, 24, 139–147.
- Lassabatere, L., Angulo-Jaramillo, R., Soria Ugalde, J.M., Cuenca, R., Braud, I., Haverkamp, R., 2006. Beerkan estimation of soil transfer parameters through infiltration experiments—BEST. *Soil Science Society of America Journal*, 70, 521. <https://doi.org/10.2136/sssaj2005.0026>
- Lassabatere, L., Angulo-Jaramillo, R., Soria-Ugalde, J.M., Šimůnek, J., Haverkamp, R., 2009. Numerical evaluation of a set of analytical infiltration equations. *Water Resources Research*, 45, W12415. <https://doi.org/10.1029/2009WR007941>
- Lassabatere, L., Angulo-Jaramillo, R., Goutaland, D., Letellier, L., Gaudet, J.P., Winiarski, T., Delolme, C., 2010. Effect of the settlement of sediments on water infiltration in two urban

- infiltration basins. *Geoderma*, 156, 316–325. <https://doi.org/10.1016/j.geoderma.2010.02.031>
- Lassabatere, L., Yilmaz, D., Peyrard, X., Peyneau, P.E., Lenoir, T., Šimůnek, J., Angulo-Jaramillo, R., 2014. New analytical model for cumulative infiltration into dual-permeability soils. *Vadose Zone Journal*, 13, 12. <https://doi.org/10.2136/vzj2013.10.0181>
- Lee, D.M., Elrick, D.E., Reynolds, W.D., Clothier, B.E., 1985. A comparison of three field methods for measuring saturated hydraulic conductivity. *Canadian Journal of Soil Science*, 65, 563–573.
- Levy, G., Shainberg, I., Morin, J., 1986. Factors affecting the stability of soil crusts in subsequent storms. *Soil Science Society of America Journal*, 50, 196–201. <https://doi.org/10.2136/sssaj1986.03615995005000010037x>
- Mualem, Y., Assouline, S., Rohdenburg, H., 1990. Rainfall induced soil seal (A) A critical review of observations and models. *Catena*, 17, 185–203.
- Mubarak, I., Mailhol, J.C., Angulo-Jaramillo, R., Ruelle, P., Boivin, P., Khaledian, M., 2009. Temporal variability in soil hydraulic properties under drip irrigation. *Geoderma*, 150, 158–165. <https://doi.org/10.1016/j.geoderma.2009.01.022>
- Mubarak, I., Angulo-Jaramillo, R., Mailhol, J.C., Ruelle, P., Khaledian, M., Vauclin, M., 2010. Spatial analysis of soil surface hydraulic properties: Is infiltration method dependent? *Agricultural Water Management*, 97, 1517–1526. <https://doi.org/10.1016/j.agwat.2010.05.005>
- Nasta, P., Lassabatere, L., Kandelous, M.M., Šimůnek, J., Angulo-Jaramillo, R., 2012. Analysis of the role of tortuosity and infiltration constants in the Beerkan method. *Soil Science Society of America Journal*, 76, 1999–2005.
- Pare, N., Andrieux, P., Louchart, X., Biarnes, A., Voltz, M., 2011. Predicting the spatio-temporal dynamic of soil surface characteristics after tillage. *Soil and Tillage Research*, 114, 135–145. <https://doi.org/10.1016/j.still.2011.04.003>
- Reynolds, W., 2008. Saturated hydraulic properties: ring infiltrometer. In: Carter, M.R., Gregorich, E.G. (Eds.): *Soil Sampling and Methods of Analysis*. 2nd ed. CRC Press, Boca Raton, pp. 1043–1056.
- Reynolds, W.D., Elrick, D.E., 1990. Ponded infiltration from a single ring: I. Analysis of steady flow. *Soil Science Society of America Journal*, 54, 1233. <https://doi.org/10.2136/sssaj1990.03615995005400050006x>
- Reynolds, W., Elrick, D., 2002. Pressure infiltrometer. In: Dane, J.H., Topp, C. (Eds.): *Methods of Soil Analysis, Part 4*. SSSA Book Series. Soil Science Society of America, American Society of Agronomy, pp. 826–836.
- Reynolds, W.D., Elrick, D.E., 2005. Chapter 6 Measurement and characterization of soil hydraulic properties. In: Álvarez-Benedí, J., Muñoz-Carpena, R. (Eds.): *Soil-Water-Solute Process Characterization – An Integrated Approach*. CRC Press, Boca Raton Römken, M., 1979. Soil crusting: when crusts form and quantifying their effects [Soil hydraulic properties]. *Agricultural Reviews and Manuals ARM NC*.
- Römken, M., Prasad, S., Parlange, J., 1990. Surface seal development in relation to rainstorm intensity. *Catena*, Supplement, 17, 1–11.
- Rose, C., 1960. Soil detachment caused by rainfall. *Soil Science*, 89, 28–35.
- Smith, R.E., 1990. Analysis of infiltration through a two-layer soil profile. *Soil Science Society of America Journal*, 54, 1219–1227. <https://doi.org/10.2136/sssaj1990.03615995005400050004x>
- Souza, E.S., Antonino, A.C.D., Heck, R.J., Montenegro, S.M.G.L., Lima, J.R.S., Sampaio, E.V.S.B., Angulo-Jaramillo, R., Vauclin, M., 2014. Effect of crusting on the physical and hydraulic properties of a soil cropped with Castor beans (*Ricinus communis* L.) in the northeastern region of Brazil. *Soil and Tillage Research*, 141, 55–61. <https://doi.org/10.1016/j.still.2014.04.004>
- van Genuchten, M.T., 1980. A closed-form equation for predicting the hydraulic conductivity of unsaturated soils. *Soil Science Society of America Journal*, 44, 892–898.
- Vandervaere, J.-P., Peugeot, C., Vauclin, M., Angulo Jaramillo, R., Lebel, T., 1997. Estimating hydraulic conductivity of crusted soils using disc infiltrometers and minitensiometers. *Journal of Hydrology, HAPEX-Sahel* 188–189, 203–223. [https://doi.org/10.1016/S0022-1694\(96\)03160-5](https://doi.org/10.1016/S0022-1694(96)03160-5)
- Warrick, A.W., 1998. Spatial variability. In: Hillel, D. (Ed.): *Environmental Soil Physics*. Academic Press, San Diego, CA, pp. 655–675.
- West, L., Chiang, S., Norton, L., 1992. The morphology of surface crusts. *Soil Crusting: Chemical and Physical Processes*, 301–308.
- Xu, X., Kiely, G., Lewis, C., 2009. Estimation and analysis of soil hydraulic properties through infiltration experiments: comparison of BEST and DL fitting methods. *Soil Use and Management* 25, 354–361. <https://doi.org/10.1111/j.1475-2743.2009.00218.x>
- Yilmaz, D., Lassabatere, L., Angulo-Jaramillo, R., Deneele, D., Legret, M., 2010. Hydrodynamic characterization of basic oxygen furnace slag through an adapted BEST method. *Vadose Zone Journal*, 9, 107. <https://doi.org/10.2136/vzj2009.0039>
- Yilmaz, D., Lassabatere, L., Deneele, D., Angulo-Jaramillo, R., Legret, M., 2013. Influence of carbonation on the microstructure and hydraulic properties of a basic oxygen furnace slag. *Vadose Zone Journal*, 12. <https://doi.org/10.2136/vzj2012.0121>

Received 23 June 2017

Accepted 15 February 2018